

# Spatially-Coupled Random Access on Graphs

Gianluigi Liva, Enrico Paolini, Michael Lentmaier and Marco Chiani

**Abstract**—In this paper we investigate the effect of spatial coupling applied to the recently-proposed coded slotted ALOHA (CSA) random access protocol. Thanks to the bridge between the graphical model describing the iterative interference cancellation process of CSA over the random access frame and the erasure recovery process of low-density parity-check (LDPC) codes over the binary erasure channel (BEC), we propose an access protocol which is inspired by the convolutional LDPC code construction. The proposed protocol exploits the terminations of its graphical model to achieve the spatial coupling effect, attaining performance close to the theoretical limits of CSA. As for the convolutional LDPC code case, large iterative decoding thresholds are obtained by simply increasing the density of the graph. We show that the threshold saturation effect takes place by defining a suitable counterpart of the maximum-a-posteriori decoding threshold of spatially-coupled LDPC code ensembles. In the asymptotic setting, the proposed scheme allows sustaining a traffic close to 1 [packets/slot].

## I. INTRODUCTION

Since the introduction of the ALOHA protocol [1], several random access (RA) schemes have been introduced. Among them, some feedback-free RA protocols originally proposed in [2], [3] re-gained attention in the recent past [4], [5]. In [2], the capacity of the so-called collision channel without feedback (CCw/oFB) was analyzed, assuming slot-aligned but completely asynchronous users' transmissions. Moreover, a simple approach to achieve error-free transmission (in noise-free setting) over the CCw/oFB was proposed. In the context of the CCw/oFB, the capacity is defined as maximum packet transmission rate per slot, which allows the receiver to recover the packets with an arbitrarily-small error probability (in noise-free conditions).

The approach of [2] consists of assigning different periodic protocol (access) sequences to the users. Each sequence defines in which slots each user is allowed to access the shared channel. Furthermore, the users encode their packets by means of erasure correcting codes. The user's packet can be recovered whenever a sufficient number of codeword segments are received collision free. Hence, by selecting proper protocol sequences, it is possible to ensure that a sufficient number of segments per user are recovered, even if the beginning of the different protocol sequences is unsynchronized. In this way, a symmetric capacity<sup>1</sup> equal to  $1/e$  [packets/slot] is achieved

Gianluigi Liva is with Institute of Communication and Navigation of the Deutsches Zentrum für Luft- und Raumfahrt (DLR), 82234 Wessling, Germany (e-mail: Gianluigi.Liva@dlr.de).

Enrico Paolini and Marco Chiani are with DEIS/WiLAB, University of Bologna, 47023 Cesena (FC), Italy (e-mail: {e.paolini, marco.chiani}@unibo.it).

Michael Lentmaier is with the Vodafone Chair Mobile Communications Systems, Dresden University of Technology (TU Dresden), D-01062 Dresden, Germany (e-mail: Michael.Lentmaier@ifn.et.tu-dresden.de).

<sup>1</sup>The symmetric capacity is given by the sum-rate capacity under the hypothesis that all users adopt the same transmission rate.

as  $N \rightarrow \infty$ , where  $N$  is the number of users accessing the RA channel. The same capacity is achieved also in the unslotted case. Although simple, the approach of [2] poses some challenges, especially if a large (and varying) number of users has to be served [3], [4].

Recently, RA schemes profiting from successive interference cancellation (SIC) have been introduced and analyzed [6]–[9]. These schemes share the feature of canceling the interference caused by collided packets on the slots where they have been transmitted whenever a clean (uncollided) copy of them is detected. In [8], [9] it was shown that the SIC process can be well modeled by means of a bipartite graph. The analysis proposed in [8], [9] resembles density evolution analysis of low-density parity-check (LDPC) and doubly-generalized LDPC (D-GLDPC) codes over erasure channels [10]–[12]. By exploiting design techniques from the LDPC context, a remarkably-high capacity (e.g. up to  $0.8$  [packets/slot]) can be achieved in practical implementations. The schemes considered in [6]–[8] assume a feedback from the receiver to achieve a zero packet loss rate.

A scheme based on the coded slotted ALOHA (CSA) of [9] has been analyzed in the context of the CCw/oFB in [13]. In [13] an upper bound on the maximum load  $G$  sustainable at a scheme rate  $R$ , has been derived as the unique positive solution to

$$G = 1 - e^{-G/R} \quad (1)$$

in  $[0, 1)$ . Still in [13] it was shown how this bound can be tightly approached by a careful selection of the distribution of the codes to be used at users for encoding their packets.

In this paper, we propose another means for approaching the bound defined by (1), which is based on spatial coupling. Spatial coupling effects were initially devised in the context of density evolution analysis of convolutional LDPC codes over the binary erasure channel (BEC) [14]–[17] and the additive white Gaussian noise (AWGN) channel [18]. Subsequently, its application to other settings relying on sparse graph representations has been investigated (see e.g. [19]–[21]). By imposing some constraints on the CSA access scheme, we show how the threshold under the iterative (IT) SIC process saturates towards a suitably-defined equivalent of the maximum-a-posteriori (MAP) decoding threshold of LDPC ensembles.

## II. CODED SLOTTED ALOHA: ERASURE DECODING MODEL

We recall next the basic model adopted for the description of CSA. We consider a slotted RA scheme where slots are grouped in medium access control (MAC) frames, all with the same length (in slots). Each user is frame- and slot-synchronous, and attempts at most one *burst* (i.e., packet) transmission per MAC frame. Each burst has a time duration

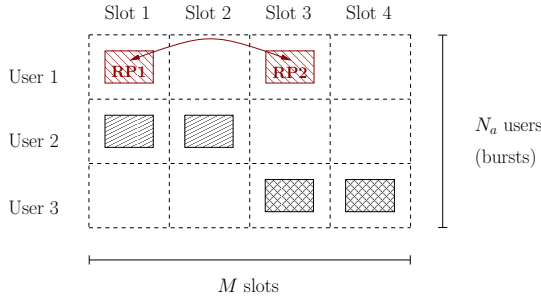


Fig. 1. MAC frame composed by  $M = 4$  slots with  $N_a = 3$  users attempting a transmission. Repetition rate  $d = 2$ .

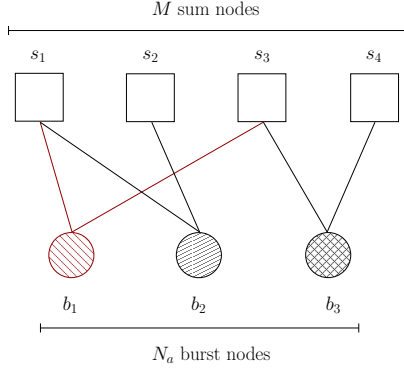


Fig. 2. Residual graph representation for the MAC frame of Fig. 1.

$T_{\text{slot}}$ , whereas the MAC frame is of time duration  $T_{\text{frame}}$ . Neglecting guard times, the MAC frame is composed of  $M = T_{\text{frame}}/T_{\text{slot}}$  slots. We consider a population of  $N$  users, with  $N \gg M$ . Users are characterized by a *sporadic* activity, i.e., at the beginning of a MAC frame each user generates a burst to be transmitted within the MAC frame with probability  $\epsilon \ll 1$ , where  $\epsilon$  is called *activation probability*. Users attempting the transmission within a MAC frame are referred to as *active* users. On the contrary, users that are idle during a MAC frame are referred to as *inactive* users. We denote the population size normalized to the frame size by  $\alpha = N/M$ . The number of active users is modeled by the random variable  $N_a$ , which is binomially-distributed with mean value  $\mathbb{E}[N_a] = N\epsilon$ . We say that the average offered channel traffic (representing the average number of bursts transmissions per slot) is

$$G = \mathbb{E}[N_a]/M = \epsilon N/M = \epsilon\alpha.$$

We consider a CSA scheme based on  $(d, 1)$  repetition codes, which is equivalent to a  $d$ -regular contention resolution diversity slotted ALOHA (CRDSA) scheme [6]. More specifically, at the beginning of a MAC frame, each user selects  $d$  slots with a uniform probability out of the  $M$  frame slots. If the user is active, it transmits  $d$  copies of its burst in the  $d$  selected slots. We define  $R = 1/d$  as the rate of the scheme. In each burst replica, a pointer to the position of the other copies is included, e.g., in a dedicated header field. Whenever a *clean* burst (i.e., a burst which did not collide) is successfully decoded, the pointer is used to determine the slots where its copies have

been transmitted. Supposing that another replica of this burst has collided, it is possible to subtract, from the signal received in the corresponding slot, the interference contribution of the twin burst. This may allow the decoding of another burst transmitted in the same slot. The SIC proceeds iteratively, i.e., *cleaned* bursts may allow solving other collisions. An example of a MAC frame with  $M = 4$  slots and  $N_a = 3$  active users is depicted in Fig. 1, where the repetition rate is  $d = 2$ .

Considering a MAC frame composed of  $M$  slots and a population of  $N = \alpha M$  users, the frame status can be described by a bipartite graph,  $\mathcal{G} = (B, S, E)$ , consisting of a set  $B$  of  $N$  *burst nodes* (one for each user), a set  $S$  of  $M$  *sum nodes* (one for each slot in the frame), and a set  $E$  of edges. An edge connects a burst node (BN)  $b_i \in B$  to a sum node (SN)  $s_j \in S$  if and only if the  $j$ -th slot has been selected by the  $i$ -th user at the beginning of the MAC frame. The graph obtained by expurgating from  $\mathcal{G}$  the BNs associated with inactive users and their adjacent edges is called the *residual graph* and is denoted by  $\mathcal{G}_a = (B_a, S, E_a)$ . Here,  $B_a \subseteq B$  is the subset of BNs associated with the active users, and  $E_a \subseteq E$  is the subset of the edges associated with the transmitted burst copies. An example of the residual graph representing the MAC frame of Fig. 1 is given in Fig. 2.

The SIC process can be represented through a message-passing along the edges of the graph. As in [6], [8], we make use of two assumptions which allows simplifying the SIC process analysis in the graphical model. First, we assume that perfect SIC is performed. Second, we claim that, whenever a clean (collision-free) burst is present in a slot, decoding succeeds with a probability that is essentially 1. It has been shown in [6], [8] that these assumptions are accurate enough to model the SIC process down to low signal-to-noise ratios (SNRs) with moderate-complexity signal processing algorithms.

Thanks to this simplification, the SIC procedure is equivalent to iterative decoding of an LDPC code with  $N$  variable nodes and  $M$  check nodes over a BEC with erasure probability  $\epsilon$  (coinciding with the activation probability). All variable nodes have degree  $d$ , while the check node degrees follow a Poisson distribution [8] with average degree  $dN/M = d\alpha$ . The *nominal code rate* is thus  $R_0 = 1 - M/N = 1 - 1/\alpha$ .

For large frames ( $M \rightarrow \infty$ ) and for a given normalized population size  $\alpha$ , CSA shows a threshold behavior. For an activation probability  $\epsilon$  lower than a threshold value  $\epsilon_{\text{block}}^{\text{IT}}$ <sup>2</sup>, vanishing burst error probability can be achieved by iterating SIC. The threshold  $\epsilon_{\text{block}}^{\text{IT}}$  can be analyzed via density evolution over the residual graph  $\mathcal{G}_a$  according to the recursions

$$q_\ell = p_{\ell-1}^{d-1} \quad (2)$$

$$p_\ell = \sum_h \tilde{\rho}_h \left( 1 - (1 - q_\ell)^{h-1} \right) = 1 - \tilde{\rho}(1 - q_\ell), \quad (3)$$

where  $\tilde{\rho}_h$  is the fraction of edges in  $\mathcal{G}_a$  connected to SNs with degree  $h$  in the residual code graph, and  $\tilde{\rho}(x) = \sum_h \tilde{\rho}_h x^{h-1}$ . In (2) and (3),  $q_\ell$  and  $p_\ell$  denote the probabilities that an edge in the residual graph carries an erasure outgoing from a BN

<sup>2</sup>The subscript ‘‘block’’ is here used to emphasize the block-structure of the MAC frame, in contrast with the spatially-coupled structure introduced in Section III.

and from a SN, respectively, at the  $\ell$ -th iteration. Since the number of collisions in a slot follows a Poisson distribution, we have

$$\tilde{\rho}(x) = e^{-\epsilon\alpha d(1-x)}. \quad (4)$$

Thus, the threshold  $\epsilon_{\text{block}}^{\text{IT}}$  is given by the supremum of the set of  $\epsilon > 0$  such that

$$q > (1 - e^{-q\epsilon\alpha d})^{d-1} \quad \forall q \in (0, 1]. \quad (5)$$

The threshold can be expressed equivalently in terms of offered traffic. By recalling that  $G = \epsilon\alpha$ , the threshold  $G_{\text{block}}^{\text{IT}}$  is given by the supremum of the set of  $G > 0$  such that

$$q > (1 - e^{-qGd})^{d-1} \quad \forall q \in (0, 1], \quad (6)$$

and we have  $G_{\text{block}}^{\text{IT}} = \epsilon_{\text{block}}^{\text{IT}}\alpha$ .

### III. SPATIALLY-COUPLED CSA: ACCESS MODEL AND DENSITY EVOLUTION

In this section, we modify the access rules of CSA to implement a convolutional-oriented structure that enables the exploitation of the spatial coupling effect.

#### A. Access Model

The modified access rules are summarized next (see also Fig. 3). A super-frame is divided into  $M_f = l+d-1$  frames of  $M$  slots each. The slots belonging to the same frame constitute a slot type set. A user becoming active at the beginning of a frame (with probability  $\epsilon$ ) transmits a burst in a slot picked uniformly at random within that frame. Furthermore, a copy of the burst is sent in each of the following  $d-1$  frames in a slot picked with uniform probability in each frame. The set of users becoming active at the beginning of the  $i$ -th frame is referred to as the type- $i$  user set. Similarly, the slots belonging to the  $j$ -th frame are referred to as type- $j$  slots. The expected size of a user set is  $\mathbb{E}[N_u] = \epsilon N$ . Thus, as before we can define the offered traffic  $G$  as  $G = \mathbb{E}[N_u]/M = \epsilon N/M$ .

After transmission of the  $l$ -th frame, transmissions from new users are forbidden, and the following  $d-1$  frames are filled just with the copies of the bursts whose transmissions have been initiated during the past  $d-1$  frames. Once all the burst copies have been transmitted, a new transmission cycle begins, i.e., a new super-frame is initialized.

A (residual) bipartite graph description of the recovery process is obtained as follows. We associate a BN to each user. Similarly, we associate a SN to each slot. The BNs corresponding to users of type  $i$  are clustered in type- $i$  BN groups, whereas the SNs related to slots of type  $i$  are clustered in type- $i$  SN groups. The number of BN types connected to a SN type- $j$  group is denoted by  $\delta_j$  (degree of the type- $j$  SN group). Note that  $\delta_j \in \{1, \dots, d\}$ . The type- $i$  BN group is said to be neighbor of a type- $j$  SN group (and viceversa) when the nodes belonging to the type- $i$  BN group are connected to some nodes in the type- $j$  SN group. The indexes of the groups that are neighbors of the type- $j$  SN group form the set  $\mathcal{N}_j^s$ , while the indexes of the groups that are neighbors of the type- $i$  BN group form the set  $\mathcal{N}_i^b$ . Note that the period in which new user transmissions are blocked is equivalent to the

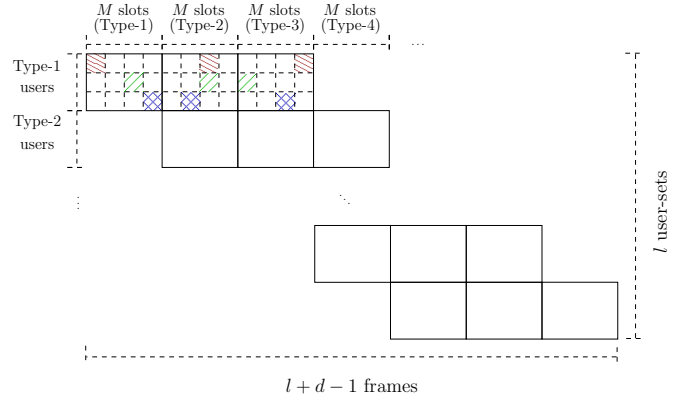


Fig. 3. Example of a convolutional super-frame structure with 3 users per user type and  $M = 4$  slots per frame.

termination in the context of convolutional LDPC codes.<sup>3</sup> An example of a super-frame structure is displayed in Fig. 3. The bursts transmitted into termination frames experience a lower collision probability than the other bursts, thus bootstrapping the iterative decoding process through the coupled structure.

#### B. Density Evolution

Let  $p_j$  be the probability that an edge incident on the type- $j$  SN group carries an erasure message towards the BNs, after SN processing at the generic SIC iteration. Analogously, let  $q_j$  be the probability that an edge incident on the type- $j$  SN group carries an erasure message towards the type- $j$  SNs, after BN processing at the generic SIC iteration. Moreover, let  $q_{i \rightarrow j}$  be the probability that an edge emanating from the type- $i$  BN group carries an erasure message towards the type- $j$  SN group (with  $j \in \mathcal{N}_i^b$ ), after BN processing at the generic SIC iteration. The physical load (i.e., the load including burst copies) for the  $i$ -th sub-frame is given by  $G^{(i)} = G \cdot \delta_i$ .

Next, we define SN degree distributions from an edge perspective as

$$\begin{aligned} \rho^{(j)}(x) &= \sum_{t=0}^{\infty} \rho_t^{(j)} x^{t-1} \\ &= \exp(-G\delta_j(1-x)) \end{aligned}$$

where  $\rho_t^{(j)}$  is the fraction of the edges emanating from type- $j$  SNs and incident on type- $j$  SNs with degree  $t$ . Density evolution equations can be now derived as follows, where  $\ell$  is the iteration index. For the type- $j$  SN group we have

$$p_{j,\ell} = 1 - \rho^{(j)}(1 - q_{j,\ell})$$

where

$$q_{j,\ell} = \frac{1}{\delta_j} \sum_{v \in \mathcal{N}_j^s} q_{v \rightarrow j,\ell}.$$

Moreover, for the type- $i$  BN group, for all  $i \in \mathcal{N}_j^b$  we have

$$q_{i \rightarrow j,\ell} = \prod_{u \in \mathcal{N}_i^b \setminus j} p_{u,\ell-1}.$$

<sup>3</sup>A loss in terms of offered traffic, with respect to  $G = \mathbb{E}[N_u]/M$ , occurs when the offered traffic is calculated taking into account the frames in which new arrivals are blocked. Nevertheless, this traffic loss is negligible for large  $l$ .

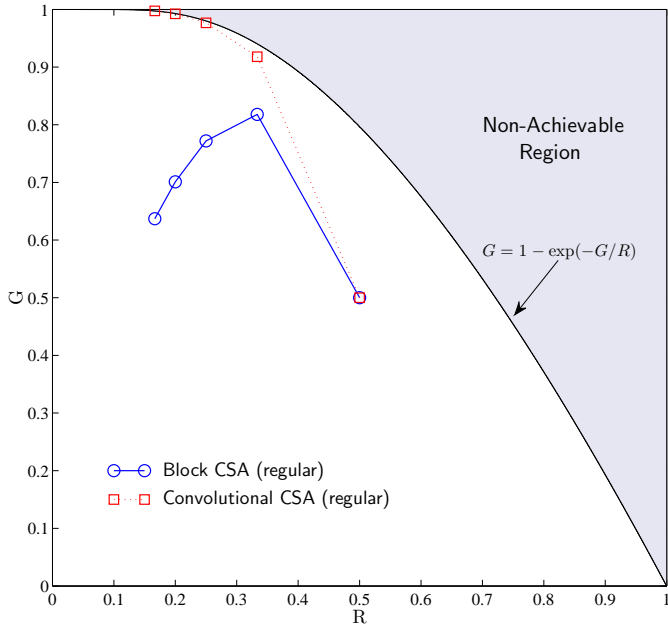


Fig. 4. Thresholds  $G_{\text{block}}^{\text{IT}}$  and  $G_{\text{conv}}^{\text{IT}}$  vs. rate,  $R = 1/d$ , for CSA based on  $(d, 1)$  repetition codes.

The SIC IT thresholds for both block-based CSA and its convolutional counterpart are plotted in Fig. 4 versus the bound (1), as functions of the rate  $R = 1/d$ . The thresholds for the spatially coupled access scheme are denoted by  $G_{\text{conv}}^{\text{IT}}$ , to emphasize the analogy with convolutional LDPC ensembles. The large SIC IT thresholds attained by the convolutional CSA scheme allow to tightly approach, already for  $d = 3$ , the limit imposed by (1). For  $d \geq 4$ , an impressive offered traffic, very close to 1 [packet/slot], can be handled by the convolutional CSA scheme with vanishing packet (i.e., burst) loss probability (in the asymptotic setting). The bound for higher rates  $R$  could be tightly approached by spatially-coupled CSA based on non-trivial  $(d, k)$  constituent codes with rate  $k/d > 1/2$  [9].

#### IV. THRESHOLD SATURATION IN CSA

We now introduce an enhanced decoding algorithm for the conventional (block) CSA case of Section II, which serves to derive an upper bound on the achievable threshold for CSA schemes, and to investigate threshold saturation effects for the convolutional scheme. This algorithm mimics the MAP decoder of an LDPC code over the BEC, and we refer to it as genie-aided maximum-a-posteriori (GA-MAP) decoder.

##### A. Genie-Aided MAP Decoding

From an analysis viewpoint, the relation between the transmitted bursts and the slot observations can be simplified by to a matrix representation of the graph via an  $M \times N_a$  binary matrix  $\mathbf{Q}$ , where  $q_{i,j} = 1$  iff BN  $b_j$  is connected to SN  $s_i$  in  $\mathcal{G}_a$ , and  $q_{i,j} = 0$  otherwise. We denote by  $\mathbf{u}$  the length- $N_a$  binary vector whose  $j$ -th element  $u_j$  is associated with the modulated burst of user  $j$ . We also denote by  $\mathbf{y}$  the length- $M$

binary vector whose  $i$ -th element is associated with the  $i$ -th slot. An equation system relating  $\mathbf{u}$  and  $\mathbf{y}$  is thus

$$\mathbf{u}\mathbf{Q}^T = \mathbf{y}. \quad (7)$$

In this simplified setting, the elements of  $\mathbf{u}$  and  $\mathbf{y}$  are binary digits which provide abstraction of the actual bursts transmitted by the users and the signals received in the slots, respectively. Upon receiving  $\mathbf{y}$  and assuming that  $\mathbf{Q}$  is revealed by a genie, the GA-MAP decoder solves (7) for  $\mathbf{u}$  via Gauss-Jordan elimination (GJE). Note that the iterative decoding process described in Section II succeeds only if the matrix  $\mathbf{Q}$  can be posed in triangular form by row/column permutations, i.e., only if the equation system (7) can be solved iteratively. Thus, the GA-MAP decoder performance (which is optimum with respect to (7)) provides a lower bound on the decoding error probability of the iterative SIC process.

##### B. CSA Analysis under GA-MAP Decoding

We establish next a bridge towards the MAP decoding threshold of LDPC codes under MAP decoding in order to derive the threshold of a  $d$ -regular CSA scheme under GA-MAP decoding,  $G_{\text{block}}^{\text{MAP}}$ . We define  $\mathcal{C}_{d,M,N}$  to be the ensemble of all length- $N$  codes given by the null space of an  $M \times N$  binary parity-check matrix  $\mathbf{H}$ , having constant column weight  $d$  and where the  $d$  1s in each column are placed in random positions, according to a uniform distribution. Recall that, for the codes in this ensemble, the nominal rate is given by  $R_0 = 1 - M/N$ . From a bipartite graph perspective, the graph of a code in  $\mathcal{C}_{d,M,N}$  possesses a constant variable node degree,  $d_v = d$  whereas, as  $N$  and  $M = (1 - R_0)N$  tend to infinity, the check node degree distribution follows a Poisson distribution with mean value  $\bar{d}_c = dN/M$ . The edge-oriented check node degree distribution is thus given by  $\rho(x) = \exp(-\bar{d}_c(1-x))$  [8].

Recall that the ensemble under consideration can be placed in analogy to the scheme introduced in Section II where  $N$  is the user population size,  $M$  is the number of slots per frame and  $d$  is the repetition rate for the bursts. The IT decoding threshold  $\epsilon_{\text{block}}^{\text{IT}}$  over the BEC for the ensemble  $\mathcal{C}_{d,M,N}$ ,  $N \rightarrow \infty$ , is calculated as the maximum value of the channel erasure probability  $\epsilon$  (the analogous of the activation probability, in the CSA context) for which the erasure probabilities  $q_i, p_i$  (where  $i$  is the iteration index) converge to an arbitrarily-low positive value, for  $i \rightarrow \infty$ , according to

$$p_i = \epsilon q_{i-1}^{d-1}, \quad (8)$$

$$q_i = 1 - \rho(1 - p_i) = 1 - \exp(-\bar{d}_c p_i). \quad (9)$$

The average extrinsic erasure probability  $p_e(\epsilon)$  under IT decoding is obtained finally as

$$p_e^{\text{IT}}(\epsilon) = \lim_{i \rightarrow \infty} q_i^d. \quad (10)$$

Defining an average extrinsic erasure probability function  $p_e^{\text{MAP}}(\epsilon)$  also for the MAP decoder, from the area theorem of [22] the area below  $p_e^{\text{MAP}}(\epsilon)$  equals the ensemble rate. By

TABLE I  
THRESHOLDS OF DIFFERENT ACCESS SCHEMES, COMPARED WITH THE  
UPPER BOUND  $G^*$ .

| $d$ | $G_{\text{block}}^{\text{IT}}$ | $G_{\text{conv}}^{\text{IT}}$ | $\bar{G}_{\text{block}}^{\text{MAP}}$ | $G^*$  | $\eta$ |
|-----|--------------------------------|-------------------------------|---------------------------------------|--------|--------|
| 2   | 0.5                            | 0.5                           | 0.5                                   | 0.7969 | 0.3726 |
| 3   | 0.8184                         | 0.9179                        | 0.9179                                | 0.9405 | 0.9760 |
| 4   | 0.7722                         | 0.9767                        | 0.9767                                | 0.9802 | 0.9964 |
| 5   | 0.7017                         | 0.9924                        | 0.9924                                | 0.9931 | 0.9993 |
| 6   | 0.6370                         | 0.9973                        | 0.9973                                | 0.9975 | 0.9998 |

noting that for any  $\epsilon$ ,  $p_e^{\text{MAP}}(\epsilon) \leq p_e^{\text{IT}}(\epsilon)$ , an upper bound [23] on  $\bar{\epsilon}_{\text{block}}^{\text{MAP}}$  is given by the value  $\bar{\epsilon}_{\text{block}}^{\text{MAP}}$  such that

$$\int_{\bar{\epsilon}_{\text{block}}^{\text{MAP}}}^1 p_e^{\text{IT}}(\epsilon) d\epsilon = R_0. \quad (11)$$

This allows us also to get an upper bound on the decoding threshold for a  $d$ -regular block CSA scheme, under GA-MAP decoding. Letting  $\alpha = N/M = 1/(1 - R_0)$ , the GA-MAP threshold of CSA can be upper bounded as

$$\bar{G}_{\text{block}}^{\text{MAP}} = \alpha \bar{\epsilon}_{\text{block}}^{\text{MAP}}.$$

### C. Threshold Saturation

Table I illustrates the threshold achievable by conventional CSA schemes employing a regular distribution at the BNs based on  $(d, 1)$  repetition codes. For the spatially-coupled scheme, a super-frame composed by  $M_f = l + d - 1$  frames has been considered, with  $l = 200$ . Moreover, the normalized user population size is  $\alpha = 100$ , i.e. the number of users is 100 times larger than the number of slots per frame. We additionally provide the upper bounds on the threshold achievable by the conventional CSA scheme under the GA-MAP recovery process. The derivation of the MAP thresholds serves to illustrate how, also in this context, the imposition of a convolutional-like structure to the access scheme allows achieving the threshold saturation effect as numerically shown in Table I. The upper bound on the achievable threshold  $G^*$  according to (1), given by the solution of  $G = 1 - \exp(-G/R)$ , is provided too. Accordingly, we evaluated the normalized efficiency of the proposed scheme as

$$\eta = G_{\text{conv}}^{\text{IT}}/G^*.$$

As already observed in the LDPC context, larger degrees allow to approach the bound more tightly.

### V. CONCLUSION

In this paper we introduced a spatially-coupled RA scheme for the CCw/oFB which attains capacities close to 1 [packet/slot] in the asymptotic (i.e., for large frames) setting. A bridge between the graphical model describing the iterative interference cancellation process of the proposed RA over the random access frame and the erasure recovery process of low-density parity-check codes over the binary erasure channel has been set, which allows computing an upper bound on the capacity achievable by an enhanced (genie-aided) decoder. The saturation of the SIC IT capacity of the proposed scheme towards the threshold under genie-aided decoding has been numerically demonstrated.

### REFERENCES

- [1] N. Abramson, "The ALOHA system - another alternative for computer communications," in *Proc. 1970 Fall Joint Computer Conference*, vol. 37. AFIPS Press, 1970, pp. 281–285.
- [2] J. L. Massey and P. Mathys, "The collision channel without feedback," *IEEE Trans. Inf. Theory*, vol. IT-31, no. 2, pp. 192–204, Mar. 1985.
- [3] J. Y. N. Hui, "Multiple accessing for the collision channel without feedback," *IEEE Trans. Veh. Technol.*, vol. VT-33, no. 3, pp. 191–198, Aug. 1984.
- [4] G. Thomas, "Capacity of the wireless packet collision channel without feedback," *IEEE Trans. Inf. Theory*, vol. 46, no. 3, pp. 1141–1144, May 2000.
- [5] K. W. Shum, C. S. Chen, C. W. Sung, and W. S. Wong, "Shift-invariant protocol sequences for the collision channel without feedback," *IEEE Trans. Inf. Theory*, vol. 55, no. 7, pp. 3312–3322, Jul. 2009.
- [6] E. Casini, R. D. Gaudenzi, and O. del Rio Herrero, "Contention resolution diversity slotted ALOHA (CRDSA): An enhanced random access scheme for satellite access packet networks," *IEEE Trans. Wireless Commun.*, vol. 6, pp. 1408–1419, Apr. 2007.
- [7] Y. Yu and G. B. Giannakis, "High-throughput random access using successive interference cancellation in a tree algorithm," *IEEE Trans. Inf. Theory*, vol. 53, no. 12, pp. 4628–4639, Dec. 2007.
- [8] G. Liva, "Graph-based analysis and optimization of contention resolution diversity slotted ALOHA," *IEEE Trans. Commun.*, vol. 59, no. 2, pp. 477–487, Feb. 2011.
- [9] E. Paolini, G. Liva, and M. Chiani, "High throughput random access via codes on graphs: Coded slotted ALOHA," in *Proc. 2011 IEEE Int. Conf. Commun.*, Kyoto, Japan, Jun. 2011.
- [10] R. Gallager, *Low-Density Parity-Check Codes*. Cambridge, MA: M.I.T. Press, 1963.
- [11] T. Richardson and R. Urbanke, "The capacity of low-density parity-check codes under message-passing decoding," *IEEE Trans. Inf. Theory*, vol. 47, no. 2, pp. 599–618, 2001.
- [12] E. Paolini, M. Fossorier, and M. Chiani, "Generalized and doubly-generalized LDPC codes with random component codes for the binary erasure channel," *IEEE Trans. Inf. Theory*, vol. 56, no. 4, pp. 1651–1672, Apr. 2010.
- [13] E. Paolini, G. Liva, and M. Chiani, "Graph-based random access for the collision channel without feedback: Capacity bound," in *Proc. 2011 IEEE Global Telecommun. Conf.*, Houston, Texas, Dec. 2011.
- [14] A. Jimenez Felström and K. Zigangirov, "Time-varying periodic convolutional codes with low-density parity-check matrix," *IEEE Trans. Inf. Theory*, vol. 45, no. 6, pp. 2181–2191, Sep. 1999.
- [15] A. Sridharan, M. Lentmaier, D. J. Costello, Jr., and K. S. Zigangirov, "Convergence analysis of a class of LDPC convolutional codes for the erasure channel," in *Proc. 42nd Allerton Conf. Commun., Control, and Computing*, Monticello, IL, Oct. 2004, pp. 953–962.
- [16] S. Kudekar, T. Richardson, and R. Urbanke, "Threshold saturation via spatial coupling: Why convolutional LDPC ensembles perform so well over the BEC," *IEEE Trans. Inf. Theory*, vol. 57, no. 2, pp. 803–834, Feb. 2011.
- [17] M. Lentmaier and G. P. Fettweis, "On the thresholds of generalized LDPC convolutional codes based on protographs," in *Proc. 2010 IEEE Int. Symp. Inf. Theory*, Austin, TX, Jun. 2010, pp. 709–713.
- [18] M. Lentmaier, A. Sridharan, D. Costello, and K. Zigangirov, "Iterative decoding threshold analysis for LDPC convolutional codes," *IEEE Trans. Inf. Theory*, vol. 56, no. 10, pp. 5274–5289, Oct. 2010.
- [19] S. Kudekar and H. Pfister, "The effect of spatial coupling on compressive sensing," in *Proc. 48th Allerton Conf. Commun., Control, and Computing*, Monticello, IL, Oct. 2010, pp. 347–353.
- [20] S. H. Hassani, N. Macris, and R. Urbanke, "Coupled graphical models and their thresholds," in *Proc. 2011 IEEE Information Theory Workshop*, Dublin, Ireland, Sep. 2010.
- [21] D. Truhachev, "Achieving AWGN channel capacity with sparse graph modulation and "in the air" coupling," in *Proc. 2012 Inf. Theory Appl. Workshop*, San Diego, CA, Feb. 2012.
- [22] A. Ashikhmin, G. Kramer, and S. ten Brink, "Extrinsic information transfer functions: Model and erasure channel properties," *IEEE Trans. Inf. Theory*, vol. 50, no. 11, pp. 2657–2673, Nov. 2004.
- [23] C. Measson, A. Montanari, and R. Urbanke, "Maxwell construction: The hidden bridge between iterative and maximum a posteriori decoding," *IEEE Trans. Inf. Theory*, vol. 54, no. 12, pp. 5277–5307, Dec. 2008.